Computers and Geotechnics 97 (2018) 62–68

Contents lists available at ScienceDirect

Computers and Geotechnics

journal homepage: www.elsevier.com/locate/compgeo

Technical Communication

Development of new prediction model for capacity of combined pile-raft foundations

Ashutosh Kumar[a], Deepankar Choudhury[b,c,*]

[a] Department of Civil Engineering, Indian Institute of Technology Bombay, Powai, Mumbai 400076, India
[b] Department of Civil Engineering, Indian Institute of Technology Bombay, IIT Bombay, Powai, Mumbai 400076, India
[c] Academy of Scientific and Innovative Research (AcSIR), CSIR Campus, India

ARTICLE INFO

Keywords:
Piled raft
Rafts
Bearing capacity
Design
Finite-element modeling

ABSTRACT

The complex soil-structure interaction factors to estimate load bearing capacity of a combined pile-raft foundation (CPRF) is scarce. A new prediction method is proposed to estimate both Ultimate Limit State (ULS) and Serviceability Limit State (SLS) bearing capacity of CPRF by evaluating the pile-raft and raft-pile interaction factors. The developed model is validated with available experimental results. The simplified expressions for the evaluation of load-sharing ratio and a mobilized factor of safety of CPRF considering the serviceability requirement of the structure are also proposed. It provides a simple design solution for CPRF subjected to vertical loading condition.

1. Introduction

For foundations of high-rise structures, the conventional pile group foundation is still dominant in the current practice which does not give credence to the raft contribution in the pile group leading to over conservatism in the design. This is due to the limited understanding of how to incorporate the capacity of both raft and piles as a single unit. There may be two cases in the design philosophy, the first one, where a raft cannot provide an adequate bearing capacity and the other one, where the raft is unable to perform under the serviceability requirement of the structure. In both the cases, the piles can be introduced below the raft to improve the safety against failure or to reduce the settlement to an acceptable level. The foundation concept where piles can be used below the raft to achieve both the safety as well as the serviceability requirements, opens up the margin of the economy in the design solution, and is called a combined pile-raft foundation (CPRF) system.

Several researchers have advocated the use of piles below the raft as settlement reducers [1–4] with some available applications [5–7]. On the other hand, few researchers have supported the bearing capacity approach if flexural rigidity of the raft is very high such that differential settlement does not pose any issue [8–10] with few available applications [11,12]. However, none of them have put forward a simplified methodology that can combine both the safety and serviceability requirements in the design philosophy.

The present study proposes an expression to estimate both the Ultimate Limit State (ULS) and the Serviceability Limit State (SLS) bearing capacity of a CPRF embedded in the medium dense sand by employing finite element methodology. The proposed expression estimates the capacity of the pile and raft components of CPRF within a maximum difference less than ± 10% when compared with the measured results. Thereafter, the simple equations to predict the load-sharing response and mobilized factor of safety considering serviceability requirement of the structure are also derived.

2. Idealisation of load-bearing mechanism of CPRF

The superstructure vertical load applied on the CPRF can be expressed in terms of load-bearing capacity. It can be computed as the summation of the capacity of pile group (*written in terms of individual pile capacities*) and un-piled raft, multiplied with their interaction factors:

$$Q_{CPRF} = \alpha_{pr}\alpha_{pp}\sum_{n=1}^{n} Q_{\text{single pile}} + \alpha_{rp}Q_{unpiled\ raft} \tag{1}$$

in which, Q_{CPRF}, $Q_{\text{single pile}}$ and $Q_{unpiled\ raft}$ are the load-bearing capacity of the CPRF, single pile and un-piled raft foundation. α_{pr}, α_{pp} and α_{rp} are pile-raft, pile-pile and raft-pile interaction factors. These factors give rise to a complex load-bearing mechanism in the CPRF, as shown in Fig. 1(a). The compatibility condition of Eq. (1) lies in equal settlement of all components of the CPRF that confirms the rigidity of the system. At the design stage, the load carrying capacity of single pile and un-piled raft are only available parameters, hence, the prediction of these

* Corresponding author at: Department of Civil Engineering, Indian Institute of Technology Bombay, IIT Bombay, Powai, Mumbai 400076, India.
E-mail addresses: ashusingh@iitb.ac.in (A. Kumar), dc@civil.iitb.ac.in, dchoudhury@iitb.ac.in (D. Choudhury).

https://doi.org/10.1016/j.compgeo.2017.12.008
Received 12 October 2017; Received in revised form 7 December 2017; Accepted 15 December 2017
0266-352X/

Nomenclature

The following symbols are used in this paper:

A_p, A_s	surface area and base area of the pile
D_P, B_r	pile diameter and raft width
E	Young's modulus
N_c, N_q and N_γ	bearing capacity factors
P_s	skin resistance along the pile shaft
q	vertical stress at the foundation level
q_b	end bearing pressure
Q_{CPRF}, $Q_{P\text{-}CPRF}$, $Q_{R\text{-}CPRF}$	load-bearing capacities of the CPRF, the piles in CPRF and raft in CPRF
$Q_{unpiled\ raft}$, $Q_{group\ piles}$	load-bearing capacities of the un-piled raft and the pile group
$Q_{single\,pile}$, $Q_{single\,pile,u}$	load-bearing and ultimate bearing capacity of the single pile
Q_r	load-carrying capacity of the raft component of the CPRF
S	pile spacing
w	settlement
α_{CPRF}	is the CPRF coefficient
α_{pp}, α_{pr}, α_{rp},	pile-pile, pile-raft and raft-pile interaction factors
ϕ	friction angle
$\overline{\tau_s}$	average limiting shear stress down the pile shaft

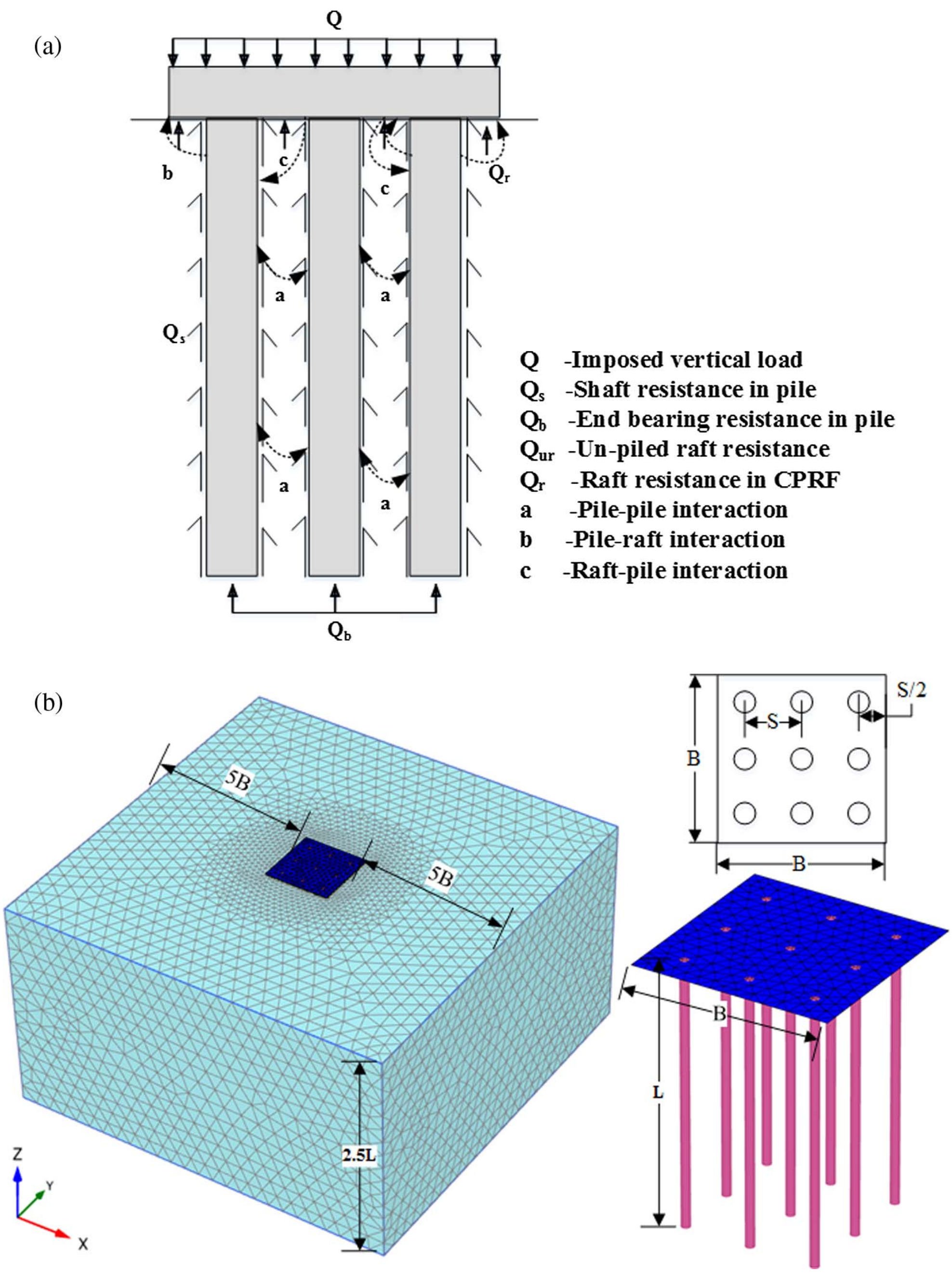

Fig. 1. Combined Pile-Raft Foundation (a) schematic representation of interaction mechanism, (b) discretised three-dimensional model.

interaction factors holds prime importance in the design. Finite element based numerical methodology is used to obtain these interaction factors.

3. Numerical simulations to obtain the interaction factors

Finite element analyses were carried out by developing three-dimensional models in PLAXIS3D [13]. The Mohr-Coulomb elastic-perfectly plastic constitutive relationship was adapted to model medium dense sand. Several researchers have used this constitutive model to simulate the behaviour of sand [7,14–17]. Mesh discretization was done by using the 10 noded tetrahedral element option available in the standard library of PLAXIS3D. Piles were modeled using the embedded beam elements with embedded interface elements to incorporate the interaction with soil along the pile depth and at the pile base, and the raft by plate elements. The rigidity of the raft was maintained by fixing the thickness of the raft as per [18]. A mesh optimization study was carried out to decide the extents of model boundaries which helped in reducing the computational effort. The dimensions of model boundaries were kept as 5 times the raft width in lateral extent and 1.5 times the pile length below the pile length in vertical extent to avoid any undesirable boundary effects. Fig. 1(b) shows the finite element discretised mesh along with the model dimensions. The geotechnical properties of the homogeneous medium dense sand and mechanical properties of piles and raft are given in Table 1. The stiffness parameters of soil dictate the load-deformation characteristics of the foundation system. The elastic modulus for medium dense sand recommended by [19] lies in the range of 25,000–50,000 kPa. In the present study, load-deformation characteristics of the pile and un-piled raft foundations are obtained for elastic modulus of 40,000 kPa to validate the hyperbolic load-deformation relationship reported by [21], as shown in Fig. 2. It was also noticed that the load-deformation characteristics obtained by using maximum and minimum values of elastic modulus range given in [19] were within the maximum difference of ±5% when compared to the results obtained for the adopted value. In addition, the negligible influence of Poisson's ratio on load-deformation characteristics of the foundation systems was also observed. This study helped in deciding the stiffness parameters of soil.

4. Validation of developed numerical model

The non-linear stress-strain behavior of soil brings non-linearity in the load-settlement response of the foundations [20]. Lee et al. [21] proposed normalized load-settlement relationship in terms of relative settlement and load, normalized with foundation size and ultimate load carrying capacity, given by:

For Pile:

$$\frac{Q_{\text{single}\,pile}}{Q_{\text{single}\,pile,\text{u}}} = \frac{w/D_p}{\alpha_p + \beta_p(w/D_p)} \tag{2}$$

For Raft:

$$\frac{Q_{unpiled\ raft}}{Q_{unpiled\ raft,\text{u}}} = \frac{w/B_r}{\alpha_r + \beta_r(w/B_r)} \tag{3}$$

where $Q_{\text{single}\,pile,\text{u}}$, $Q_{unpiled\ raft,\text{u}}$ are the ultimate bearing capacities of single pile and unpiled-raft foundation, respectively. w is the settlement level, D_p and B_r are the pile diameter and raft width. Eqs. (2) and (3) carry flexible applicability to various foundation conditions i.e. changes in the geometrical properties and local soil conditions. The model parameters α_p and β_p for pile foundation were reported as 0.01 and 0.9; and α_r, β_r for unpiled raft foundation were 0.02 and 0.8 at the settlement of 10% of the foundation width (*Limit state condition*). This settlement level was supported with experimental evidence reported by [22]; [23] on the model raft and [24]; [25] for a pile foundation.

The load-settlement response obtained through finite element methodology was compared with the normalized hyperbolic load-settlement response model proposed by [21]. The ultimate bearing capacity $Q_{unpiled\ raft,\text{u}}$ of a un-piled raft foundation was calculated on the basis of the theory of plasticity given by [26]:

$$Q_{unpiled\ raft,\text{u}} = (cN_c + qN_q + 0.5B_r\gamma N_\gamma)A \tag{4}$$

where γ is the unit weight of soil, c is the soil cohesion, q is the vertical stress at foundation level, N_c, N_q and N_γ are bearing capacity factors. The ultimate bearing capacity of the pile $Q_{\text{single}\,pile,\text{u}}$ was obtained as:

$$Q_{\text{single}\,pile,\text{u}} = \overline{\tau_s}A_s + q_bA_b \tag{5}$$

where A_s and A_b are shaft and base area of the pile, $\overline{\tau_s}$ and q_b are average limiting shear stress down the pile shaft and end-bearing pressure respectively.

Fig. 2 illustrates the comparison of the results for a 6 m wide raft ($Q_{unpiled\ raft,\text{u}}$ = 36.38MN) and 0.5 m diameter, 15 m long pile ($Q_{\text{single}\,pile,\text{u}}$ = 2434 kN) obtained by numerical methodology with the hyperbolic model proposed by [21]. It can be clearly seen that both the results are in close agreement. This confirms the qualitative and quantitative validation of the numerical model. It can be noted that the numerical model attained the displacement of 10% of the foundation width. This shows that the finite element method is well suited to predicting the collapse mechanism of geotechnical structures provided it is applied properly [27].

5. Evaluation of Interaction factors

After successful validation of the numerical model, a detailed parametric study, given in Table 2 was carried out by varying the influencing parameters for a 3 × 3 pile configuration. Thereafter, an effect of pile configurations was also studied by changing the configurations from 5 × 5 to 9 × 9 for a particular pile diameter of 0.5 m. A total of 170 numerical models were run and analyzed to achieve this goal.

5.1. Estimation of pile-pile interaction factor (α_{pp})

The pile-pile interaction is the result of pile group effect, defined as the changes in the load-settlement response of a pile group and single piles due to superimposition of stress and displacement field of a single pile in a group [28,29]. The load carrying capacity of a pile group can be expressed as load carrying capacity of a single pile using this factor:

$$Q_{group\ piles} = \alpha_{pp}\sum_{n=1}^{n} Q_{\text{single pile}} \tag{6}$$

Long [30] and Poulos [31] reported the value of unity for medium dense sand. It is also evident from the present study that pile group foundation attained ultimate capacity at the settlement level of 10% of the pile diameter. This attained capacity was equal to the ultimate capacity of the number of single piles present in the group which indicated the interaction factor of unity at higher settlement level. The settlement incurred in a CPRF is much higher than in a pile group. Hence, a pile-pile interaction factor of unity is adopted herein.

Table 1
Geotechnical properties of soil and mechanical properties pile and raft as an input parameter [19]

Parameter	Symbol/Unit	Soil	Pile/Raft
Soil unit weight	γ (kN/m^3)	18	25
Relative density	D_r (%)	50	–
Cohesion	c (kN/m^2)	0	–
Friction	ϕ	30	–
Elastic modulus	E (kN/m^2)	40,000	30,000,000
Poisson's ratio	μ	0.32	0.2
Dilation angle	ψ	0	–

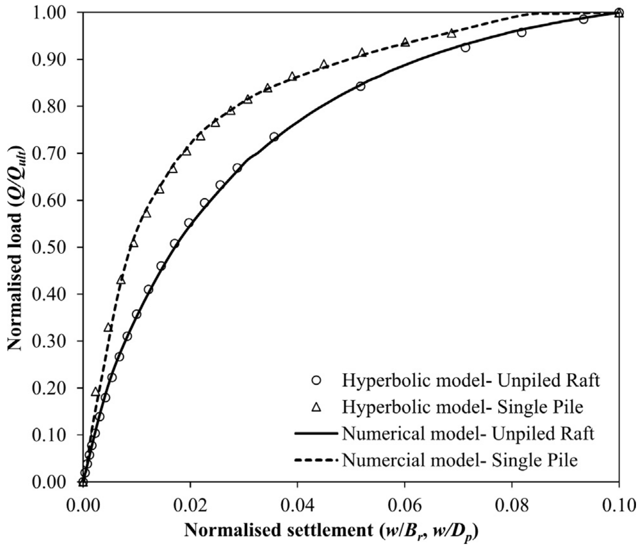

Fig. 2. Comparison of the load-sharing response obtained by hyperbolic model and numerical study.

5.2. Estimation of pile-raft interaction factor (α_{pr})

The pile-raft interaction is defined as the changes in the load-settlement response of pile group when the raft is being rested to the soil surface. The load carrying capacity of piles in CPRF Q_{P-CPRF} can be expressed as the load carrying capacity of the pile group using this interaction factor as:

$$Q_{P-CPRF} = \alpha_{pr} Q_{group\,piles} \tag{7}$$

The pile-raft interaction affects the load-settlement response of CPRF in both positive and negative aspects [5]. The positive aspect refers to the increase in the load carrying capacity of piles of CPRF due to increase in confinement of the soil mass below the raft which subsequently increases the skin resistance in the piles. This effect is primarily dependent on the location of pile within the raft. On the other hand, the negative aspect refers to lesser mobilization of pile resistance due to the lesser relative displacement between piles and surrounding soil because soils below the raft were forced to move leading to the release of confinement stress. Since, both the phenomena are dependent on the mobilization of displacement on loading, the estimation of this interaction considering both negative and positive aspects is very complex. In the present study, α_{pr} is evaluated by dividing the capacity of the group piles and pile components of CPRF at various settlement levels, as shown in Fig. 3. The values of α_{pr} is increasing with increase in the settlement level and converging to unity. This indicates that negative interaction dominates at lower settlement level and subsequently changes to positive interaction as the settlement in the CPRF increases. Negligible influence on α_{pr} with change in configuration from 3 × 3 to 9 × 9 was observed because it has been implicitly accounted in the expression. The obtained interaction factors for various configurations followed a certain trend; hence, an expression was fitted through the method of least square. The predicted values of α_{pr} were limited to unity for conservatism in the design and expressed as:

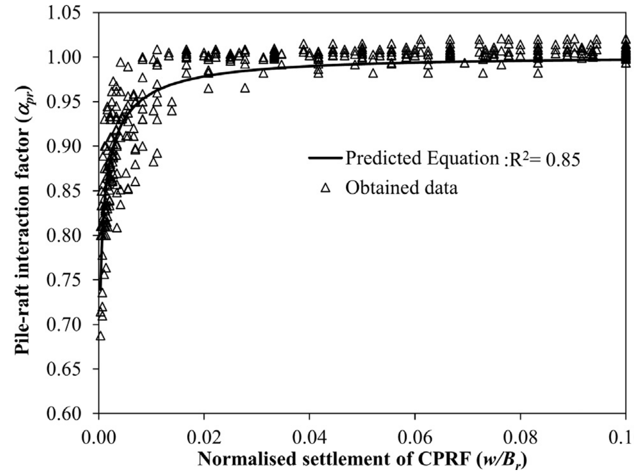

Fig. 3. Variation of pile-raft interaction factor (α_{pr}) with normalised settlement (w/B_r).

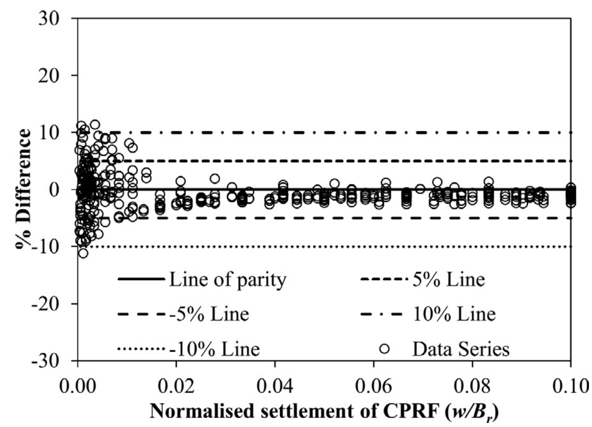

Fig. 4. Variation of percentage difference between numerically obtained results and prediction model for pile-raft interaction factor (α_{pr}).

$$\alpha_{pr} = \frac{Q_{P-CPRF}}{Q_{group\,piles}} = 1-\exp(-10.55(w/B_r)^{0.26}) \tag{8}$$

Fig. 4 illustrates the percentage difference in the results obtained by proposed expression and finite element methodology which indicates that almost all values are lying within the maximum range of ± 10%. Hence, it can be stated that the obtained capacity of piles in CPRF through the proposed expression will be in the range of ± 10% difference. The validity of the proposed expression is then examined by comparing the capacity of piles in CPRF obtained by Eq. (8) with that reported by [10]. They carried out centrifuge tests on a single pile, pile group, un-piled raft and CPRF embedded in the medium dense sand (D_r = 52%). The relative density of the medium dense sand modelled in the present study is nearly same as reported by [10]. The piles were of 0.6 m diameter and 15 m in length spaced at 2.4 m (S/D_p = 4) centre to centre with the configuration of 4 × 4 in the group pile and CPRF, at prototype scale. Please refer to [10] for further details. Fig. 5 illustrates the comparison in the load-settlement curve reported by [10] and

Table 2
Configuration chosen for the study.

Pile spacing to diameter ratio (S/d)	3	4	5	6	Pile length (m)	Pile Number
Pile diameter (m)	Raft width (m)					
0.5	4.5, 7.5, 10.5, 13.5	6, 10, 14, 18	7.5, 12.5, 17.5, 22.5	9, 15, 21, 27	10, 15, 20	9, 25, 49, 81
0.8	7.2	9.6	12	14.4	10, 15, 20	9
1	9	12	15	18	10, 15, 20	9

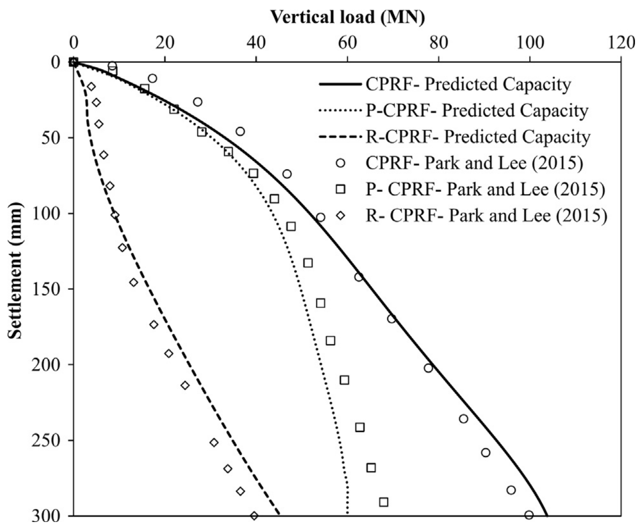

Fig. 5. Comparison of load-settlement response obtained by centrifuge study and prediction model.

predicted by the proposed equation, which ascertained the validity of the proposed expression.

5.3. Estimation of raft-pile interaction factor (α_{rp})

The raft-pile interaction is defined as the modification in the load carrying mechanism of the raft when a few piles are introduced beneath. The load carrying capacity of a raft of CPRF, Q_{R-CPRF} can be computed in terms of load carrying capacity of a un-piled raft using this factor:

$$Q_{R-CPRF} = \alpha_{rp} Q_{unpiled\ raft} \tag{9}$$

The raft-pile interaction depends on the mobilization of pile skin friction due to downward movement of soil which in turn reduces the confining stress just below the raft. To evaluate α_{rp}, one new factor called CPRF efficiency factor η is introduced. It is expressed as the ratio of load carrying capacity of CPRF to the summation of the load-bearing capacity of the un-piled raft and the pile group:

$$\eta = \frac{Q_{CPRF}}{Q_{UR} + Q_{PG}} \tag{10}$$

The value of η is calculated for all the configurations mentioned in Table 2 which indicates, an increase in η with an increase in the normalised settlement (w/B_r) as shown in Fig. 6 for a few cases. Negligible influence on η with change in configuration was observed because it has been implicitly accounted for the solution. A generalized prediction equation was fitted with the obtained results using the method of least square as:

$$\eta = 3.5(w/B_r) - 0.06(S/D_p) - 0.51D_p + 1.27 \tag{11}$$

Fig. 7 illustrates the percentage difference in the values obtained by the predicted equation and the finite element methodology which shows that most of the values are within a maximum difference of ± 10%. Thereafter, an equation of α_{rp} is derived by using η and α_{pr} as:

$$\alpha_{rp} = \frac{Q_{R-CPRF}}{Q_{unpiled\ raft}} = \eta + (\eta - \alpha_{pr})\frac{Q_{PG}}{Q_{UR}} \tag{12}$$

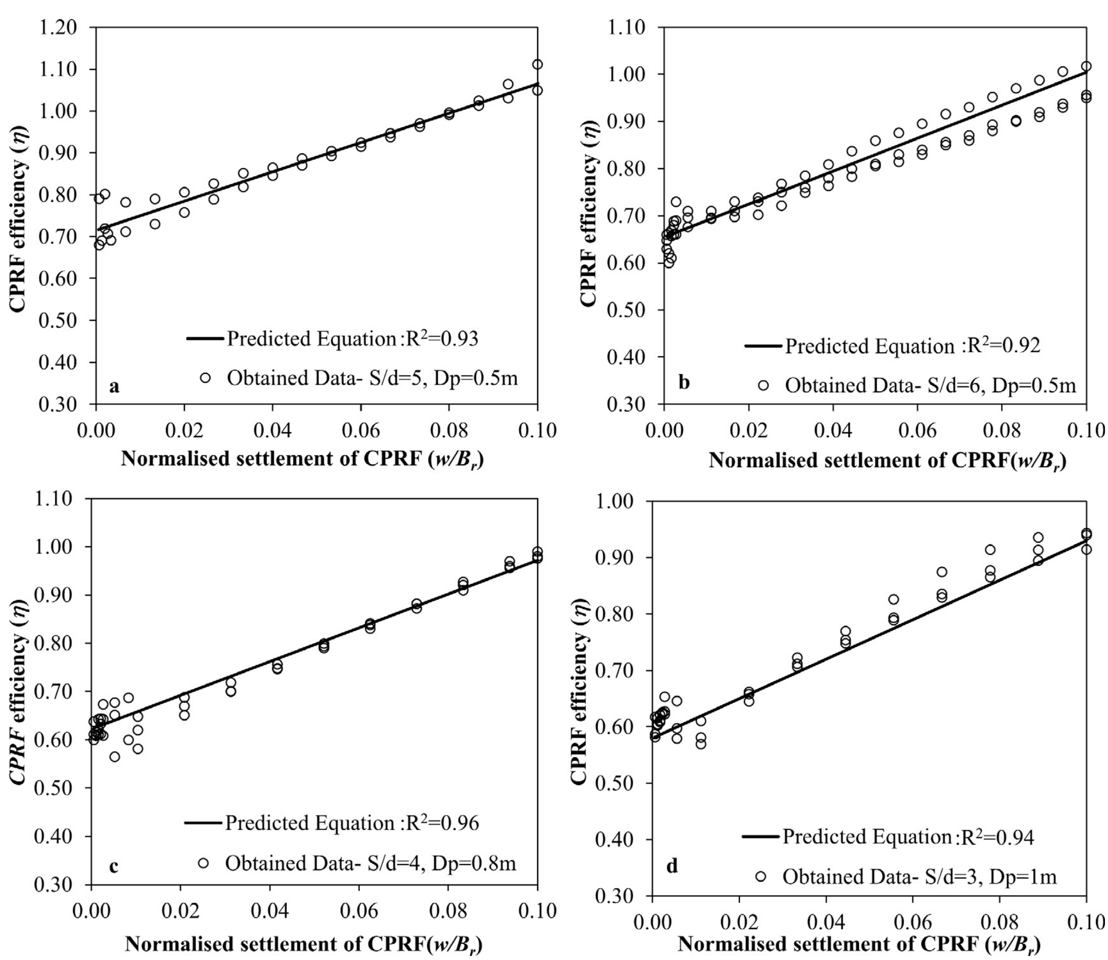

Fig. 6. Variation of CPRF efficiency (η) with normalised settlement (w/B_r) (a) $S/d = 5$ and $D_p = 0.5$ m, (b) $S/d = 6$ and $D_p = 0.5$ m, (c) $S/d = 4$ and $D_p = 0.8$ m (d) $S/d = 3$ and $D_p = 1$ m.

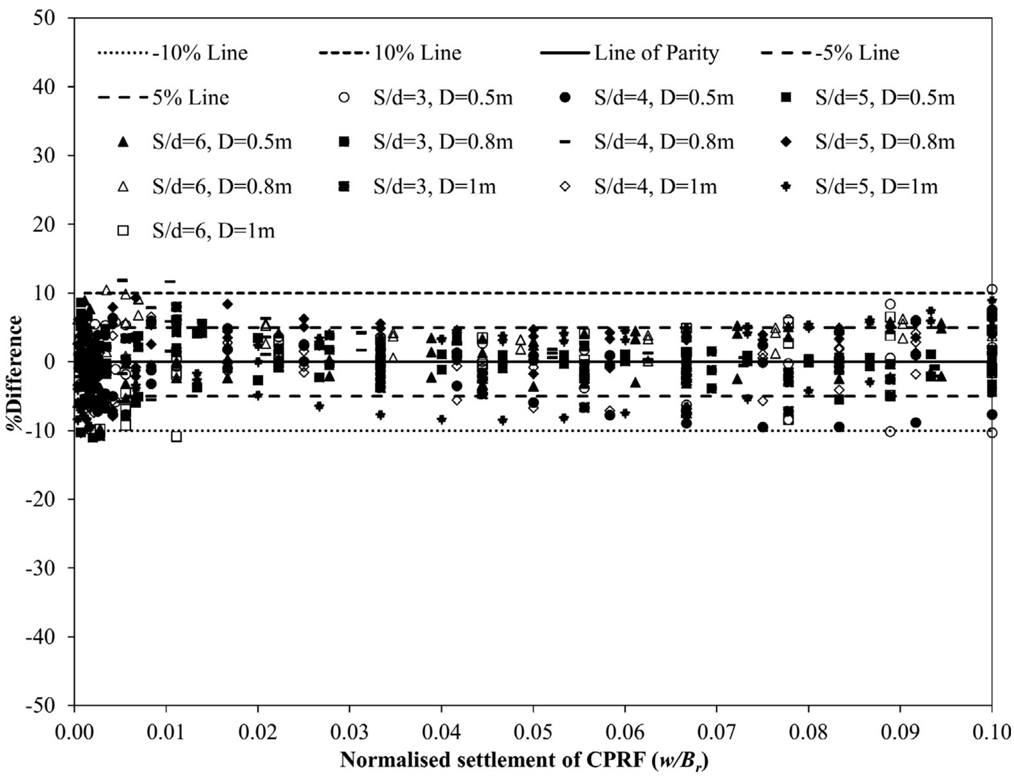

Fig. 7. Variation of percentage difference in numerically obtained results with prediction model for CPRF efficiency (η).

Thus, the capacity of CPRF, Q_{CPRF} and raft in CPRF, Q_{R-CPRF} can now be obtained by simply using the Eqs. (10)–(12). The validity of Equation was confirmed by comparing the results reported by [10], as shown in Fig. 5. Hence, it can be postulated that the (Serviceability Limit State) SLS and (Ultimate Limit State) ULS bearing capacity of CPRF can be determined by using Eqs. (2), (3) and (10). A similar methodology can be adopted for obtaining the bearing capacity of CPRF for dense sand condition, owing to the estimation of pile-raft interaction and CPRF efficiency factor.

6. Load sharing and mobilised factor of safety model of CPRF

The load sharing by CPRF components are dependent on the attainment of settlement level and hence plays a very important role in deciding the serviceability requirement of the structure. It can be expressed in terms of α_{CPRF}, defined as the ratio of load carried by piles in CPRF to the total imposed load, can be expressed as:

$$\alpha_{CPRF} = \frac{Q_{P-CPRF}}{Q_{CPRF}} = \frac{\alpha_{pr} Q_{PG}}{\eta(Q_{PG} + Q_{UR})} = \frac{\alpha_{pr}}{\eta\left(1 + \frac{Q_{UR}}{Q_{PG}}\right)} \tag{13}$$

It can also be written in terms of the hyperbolic model of piled and un-piled raft foundation as:

$$\alpha_{CPRF} = \frac{1}{\frac{\eta}{\alpha_{pr}}\left[1 + \frac{Q_{UR,u}}{Q_{PG,u}}\left(\frac{(D/B_r)\alpha_p + \beta_p(w/B_r)}{\alpha_r + \beta_r(w/B_r)}\right)\right]} \tag{14}$$

Fig. 8(a) illustrates a comparison between the variation of α_{CPRF} obtained by the numerical study and prediction model for a 3 × 3 pile configuration (15 m length, 0.5 m diameter) at $S/d = 5$. Non-linearity in the variation of load sharing response can be seen. It can also be observed that the results obtained by prediction model are matching well with the numerical model.

The evaluation of factor of safety for any geotechnical structure is a prime concern to practicing engineers. Herein, the mobilized factor of safety of CPRF, FS_{CPRF} can be obtained in terms of a factor of safeties of group piles and un-piled raft. To do this, the factor of safety of un-piled raft can be expressed for any working load as:

$$FS_{unpiled\ raft} = \frac{Q_{unpiled\ raft,u}}{Q} \tag{15}$$

The factor of safety of group pile can be expressed for any working load as:

$$FS_{grp\ pile} = \frac{Q_{group\ pile,u}}{Q} \tag{16}$$

Similarly, The Factor of safety for CPRF can be written as:

$$FS_{CPRF} = \frac{Q_{CPRF,u}}{Q} \tag{17}$$

The ratio of a factor of safeties can be expressed as:

$$\frac{FS_{CPRF}}{FS_{unpiledraft} + FS_{GRP\ Pile}} = \frac{Q_{CPRF,u}}{Q_{ubpiled\ raft,u} + Q_{Group\ pile,u}} = \eta \tag{18}$$

Hence, FS_{CPRF} can be expressed by combining the Eqs. (2), (3) and (10) as:

$$FS_{CPRF} = \eta\left(\frac{\alpha_p + \beta_p(w/D_p)}{(w/D_p)} + \frac{\alpha_r + \beta_r(w/B_r)}{(w/B_r)}\right) \tag{19}$$

Fig. 8(b) illustrates the variation of a mobilized factor of safety for CPRF with pile configuration of 5 × 5 pile configuration (15 m length, 0.5 m diameter) at $S/d = 3$. It can be observed that the results obtained by prediction model are matching well with the finite element results which support the accuracy of the new method.

7. Conclusions

This paper proposes a simplified new prediction model for the bearing capacity and efficiency evaluation for the CPRF at both SLS and ULS. Finite element modeling was used to achieve this goal. The proposed expressions were validated with the centrifuge results available in the literature. From the study, it has been found that the capacity of a CPRF and its components can be predicted at any settlement level

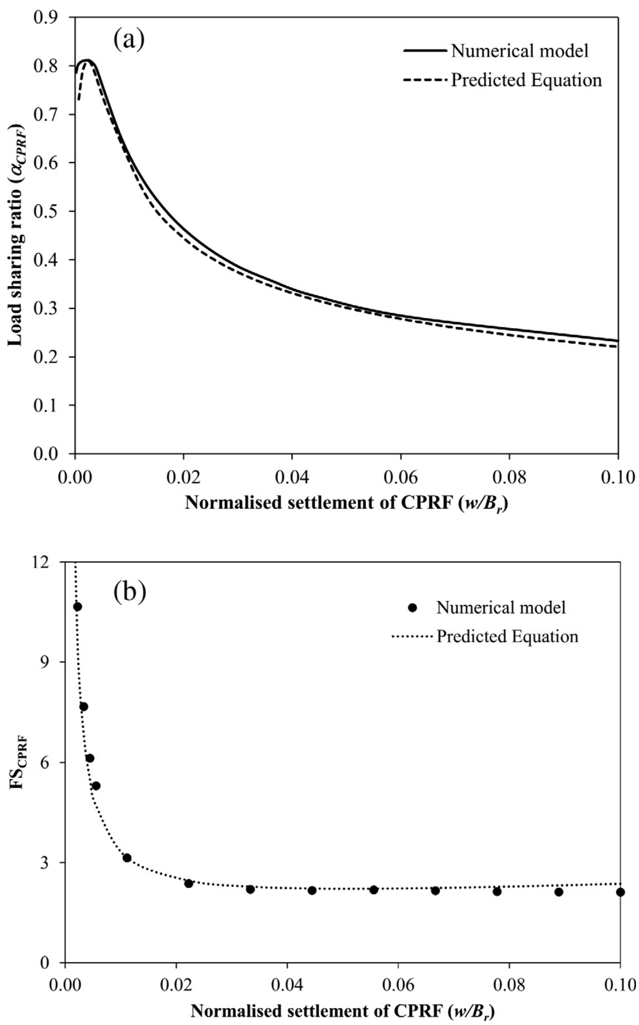

Fig. 8. Comparison between numerical study and prediction model results (a) Load sharing ratio (α_{CPRF}), (b) mobilised factor of safety (FS_{CPRF}).

provided the capacity of a pile group and an unpiled-raft foundation is known. It also outlines the estimation of load sharing ratio and mobilised factor of safety of CPRF. Thus, the proposed expressions prove to be a marked improvement over the current design practice with reasonable accuracy, which can be used in the design of a CPRF.

References

[1] Burland LB, Broms, B, de Mello VFB. Behaviour of foundations and structures. In: Proceedings of the 7th International Conference on Soil Mechanics and Foundation Engineering, Tokyo, vol. 1; 1977. p. 495–46.
[2] Hain SJ, Lee IK. The analysis of flexible pile-raft system. Geotechnique 1978;28(1):65–83.
[3] Randolph M F. Design method for pile group and piled raft. In: Proc. 13th Int Conf Soil Mech, New Delhi; 1994; 5: p. 1–21.
[4] Poulos HG. Piled raft foundations: design and applications. Géotechnique 2001;51(2):95–113.
[5] Katzenbach R, Arslan U, Moormann C. Piled raft foundation projects in Germany. Design applications of raft foundations, Hemsley. Thomas Telford, London, UK; 2000, p. 323–91.
[6] Katzenbach R, Leppla S, Choudhury D. Foundation systems for high-rise structures. UK: CRC Press, Taylor and Francis Group; 2016. p. 1–298.
[7] Kumar A, Choudhury D, Katzenbach R. Effect of earthquake on combined pile-raft foundation. Int J Geomech ASCE 2016;16(5):04016013.
[8] de Sanctis L, Mandolini A, Russo G, Viggiani C. Some remarks on the optimum design of piled rafts. In: Proc. ASCE Deep Foundations 2002: An Int Perspective on Theory, Design, Construction, and Performance, Reston, Va.; 2002. p. 405–25.
[9] de Sanctis L, Mandolini A. Bearing capacity of piled rafts on soft clay soils. J Geotech Geoenviron Eng ASCE 2006;132(12):1600–10.
[10] Park D, Lee J. Comparative analysis of various interaction effects for piled rafts in sands using centrifuge tests. J Geotech Geoenviron Eng ASCE 2015;141(1):04014082.
[11] de Sanctis L, Russo G. Analysis and performance of piled rafts designed using innovative criteria. J Geotech Geoenviron Eng ASCE 2008;134(8):1118–28.
[12] Kumar A, Patil M, Choudhury D. Soil – structure interaction in a combined pile – raft foundation – a case study. Proc ICE- Geotech Eng 2017;170(2):117–28.
[13] PLAXIS3D. Plaxis 3D User Manuals. PLAXIS BV, Delft, Netherlands; 2013.
[14] Manoharan N, Dasgupta SP. Bearing capacity of surface footings by finite elements. Comput Struct 1995;54(4):563–86.
[15] Kumar A, Choudhury D. DSSI analysis of pile foundations for an oil tank in Iraq. Proc ICE Geotech Eng 2016;169(2):129–38.
[16] Kumar A, Choudhury D. Load sharing mechanism of combined pile-raft foundation (CPRF) under seismic loads. Geotech Eng 2017;48(3):95–101.
[17] Kumar A, Choudhury D, Shukla J, Shah DL. Seismic design of pile foundation for oil tank by using PLAXIS3D. Disaster Adv 2015;8(6):33–42.
[18] Horikoshi K, Randolph MF. On the definition of raft—soil stiffness ratio for rectangular rafts. Geotechnique 1997;47(5):1055–61.
[19] Bowles JE. Foundation analysis and design. 5th ed. New York, NY, USA: McGraw-Hill; 1997.
[20] Clemente JLM. Nonlinear analysis of settlement and load distributions in pile groups. Comput Struct 1990;36(2):203–10.
[21] Lee J, Park D, Choi K. Analysis of load sharing behaviour of piled raft using normalised load response model. Comput Geotech 2014;57:65–74.
[22] Cooke RW. Piled raft foundations on stiff clays-a contribution to design philosophy. Geotechnique 1986;36(2):169–203.
[23] Lee J, Salgado R. Estimation of bearing capacity of circular footing on sands based on cone penetration test. J Geotech Geoenviron Eng ASCE 2005;131(4):442–52.
[24] Lee J, Salgado R. Determination of pile base resistance in sand. J Geotech Geoenviron Eng ASCE 1999;125(8):673–83.
[25] Cerato AB, Lutenegger AJ. Bearing capacity of square and circular footings on a finite layer of granular soil underlain by a rigid base. J Geotech Geoenviron Eng ASCE 2006;132(11):1496–501.
[26] Terzaghi K. Theoretical soil mechanics. New York: Wiley; 1943.
[27] Potts DM. Numerical analysis: a virtual dream or reality? Geotechnique 2003;53(6):535–73.
[28] Randolph MF, Wroth CP. An analysis of vertical deformation of pile groups. Geotechnique 1979;29:423–39.
[29] Chow YK. Discrete element analysis of settlement of pile groups. Comput Struct 1986;24(1):157–66.
[30] Long PD. Footings with settlement-reducing piles in non-cohesive soil. Ph.D. thesis, Chalmers University of Technology, Gothenburg, Sweden; 1993.
[31] Poulos HG. Practical design procedures for piled raft foundations. In: Hemsley JA, editor. Design applications of raft foundations. London: Thomas Tel- ford; 2000. p. 425–67.